EPJ Web of Conferences 32, 01007 (2012)
DOI: 10.1051/epjconf/20123201007

On possibility of low-threshold two-plasmon decay instability in 2nd harmonic ECRH experiments at toroidal devices

E. Z. Gusakov[1,2] and A.Yu. Popov[1,2]

[1] Ioffe Institute of RAS, 26 Polytekhnicheskaya st., St. Petersburg 194021, Russia
[2] RLPAT, St. Petersburg State Polytechnical University, 29 Polytekhnicheskaya st., St. Petersburg 195251, Russia

Abstract. The effects of the parametric decay of the 2nd harmonic X-mode into two short wave-length UH plasmons propagating in opposite directions is considered. The possibility of the absolute instability excitation is demonstrated in the case of the density profile possessing local maximum slightly exceeding the UH resonance value. The threshold of the absolute instability is shown to be substantially smaller than that provided by the standard theory for monotonous density profile.

1 INTRODUCTION

Electron cyclotron resonance heating (ECRH) at power level of up to 1 MW in a single microwave beam is widely used nowadays in tokamak experiments and is considered for application in ITER for neoclassical tearing mode island control as well. As having been revealed by theoretical analysis a couple of decades ago [1] – [3] parametric decay instabilities (PDI) which may accompany ECR fundamental harmonic ordinary (O) mode and 2nd harmonic extraordinary (X) mode heating experiments are believed to be deeply suppressed by convective losses of daughter waves both along the magnetic field and in radial direction. Thus, the EC wave propagation and absorption are thought to be well described by linear theory and predictable in detail. However, during the last decade many observations have been made evidencing presence of anomalous phenomena which accompany ECRH experiments at toroidal devices. An eloquent example of these phenomena is the backscattering effect correlated to the MHD mode rotation observed recently in the 200 – 600 kW level 2nd harmonic ECRH experiment at Textor tokamak [4].
An explanation of this effect utilizing induced backscattering PDI low-threshold onset was proposed in [5] – [8]. The threshold lowering of this direct process according to [5] – [8] occurs due to excitation of trapped ion Bernstein waves possible due to the actual Textor plasma density profile possessing the local maximum in the O-point of the magnetic island [9]. Being direct and quite natural this explanation is not unique because the backscattering signal could be produced as a result of a secondary nonlinear process accompanying a primary low-threshold PDI of a different nature. A hint to this primary instability is provided by [4, 10] demonstrating the most intensive backscattering at plasma density in the magnetic island slightly exceeding the upper hybrid (UH) resonance value for half a pump frequency.
In the present paper the effects of the parametric decay of the 2nd harmonic X-mode wave into two short wave-length UH plasmons propagating in opposite directions is considered. We demonstrate

the possibility of the 3D localization of both the UH daughter waves. Similar to the mechanism of the IB wave trapping in radial direction [5], the radial localization of the UH waves can be achieved in a vicinity of the density profile local maximum often observed in ECRH experiments at toroidal

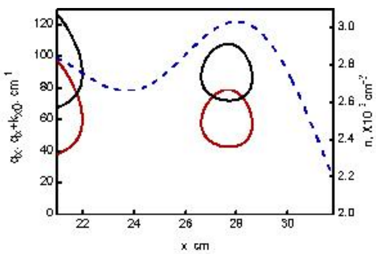

Fig. 1: (a, left and bottom axes) – 1D dispersion curves q_x (red curves) and $q_x + k_{x0}$ (black curves) defined in (5); (b, right and bottom axes) – density profile with the local max. corresponding to O-point of the magnetic island ($m = 2, n = 1$); In the points where the red and black curves intersect – Bragg resonance conditions are fulfilled, $T_e = 500eV$, $x_{ECR} = -28cm$, $2\omega_{ce}(x_{ECR}) = \omega_0$, $\omega = \omega_0 / 2$, $q_v = 0$, $k = l = 13$.

devices (at the discharge axis for the peaked profile, at the edge for the hollow density profile or at the O-point of the magnetic island). On the other hand, when the pump power is high enough, the UH waves, propagating oppositely, can be trapped in the poloidal and toroidal directions due to the finite size of the microwave beam. The 3D localization of the UH waves leads to excitation of the absolute PDI. Being derived explicitly the threshold of this absolute PDI is drastically smaller than that provided by the standard theory [1] – [3].

2 PHYSICAL MODEL

To elucidate the physics of the absolute PDI we analyze the most simple but nevertheless relevant to the experiment three wave interaction model in which the X-mode pump wave propagates almost perpendicular to the magnetic field $\vec{H} = H \cdot \vec{e}_z$ in the density inhomogenuity direction along unit vector $\vec{e}_x$ with its polarization vector being mostly directed along the poloidal direction ϑ, which almost coincides with unit vector $\vec{e}_y = \vec{e}_z \times \vec{e}_x$ direction. We represent a wide microwave beam of the X-mode pump wave propagating from the launching antenna inwards plasma along major radius in the tokamak mid-plane as

$$E_\vartheta = a_i(y,z)/2 \cdot \exp(ik_0 x - i\omega_0 t) + c.c. \tag{1}$$

where c.c. is complex conjugation, $a_i = \sqrt{8\pi / c \cdot P_0 / (\pi w^2)} \exp\left[-\left(y^2 + z^2\right)/2w^2\right]$ is the amplitude, P_0 is the pump wave power and w is the beam waist. The basic set of integral equations describing the X-mode pumping wave (1) decay into two UH waves, propagating in opposite directions, reads as

$$\begin{cases} \hat{D}(\vec{r},\vec{r}';\omega)\{\phi_1(\vec{r}')\} = 4\pi\rho_1(\vec{r};\omega)\{a_i(\vec{r}),\phi_2(\vec{r})\} \\ \hat{D}(\vec{r},\vec{r}';\omega_0-\omega)\{\phi_2(\vec{r}')\} = 4\pi\rho_2(\vec{r};\omega_0-\omega)\{a_i^*(\vec{r}),\phi_1(\vec{r})\} \end{cases} \tag{2}$$

The integral operators $\hat{D}$ in (2) are defined in weakly inhomogeneous plasma as follows:

$$\hat{D}(\vec{r},\vec{r}';\Omega)\{f(\vec{r}')\} = (2\pi)^{-3} \int_{-\infty}^{\infty} d\vec{q}d\vec{r}' D(\vec{q},\vec{r}+\vec{r}'/2;\Omega) \exp\left[i\vec{q}(\vec{r}-\vec{r}')\right] f(\vec{r}'), \tag{3}$$

where $\Omega = [\omega, \omega_0 - \omega]$, $D = l_T^2 q_\perp^4 + \varepsilon(x) q_\perp^2 + \omega^2 g^2 / c^2 + \eta q_z^2$ is a dispersion relation of the UH wave, $q_\perp^2 = q_x^2 + q_y^2$, $l_T^2 = -3\omega_{pe}^2 \upsilon_{te}^2 / \left(2(\Omega^2 - \omega_{ce}^2)(\Omega^2 - 4\omega_{ce}^2)\right)$, $g = \omega_{ce}/\Omega \cdot \omega_{pe}^2 / \left(\Omega^2 - \omega_{ce}^2\right)$, $\eta = 1 - \omega_{pe}^2 / \Omega^2$. The nonlinear induced charge densities $\rho_{1,2}(\vec{r};\Omega)$ arising in r.h.s. of (3) and describing the UH wave and the fast X-mode EC wave coupling are given by an expression:

$$\rho_j\left(\vec{r};\Omega_j\right)=-\frac{en_0}{\Omega_j}\frac{\left(\vec{q}_j\cdot\vec{u}_0\right)\left(\vec{q}_p\cdot\vec{u}_p\right)}{\Omega_j\Omega_p}\left(\Omega_j-\Omega_p\right)-\frac{k_0u_{0x}}{4\pi\omega_0}q_{xj}q_{xp}\varphi_p\left[1+\frac{3}{2}\frac{\omega_0^2}{\Omega_j^2-\omega_{ce}^2}\right],$$

$j\neq p$, $j,p=(1,2)$, where $\vec{u}_0$ and $\vec{u}_j$ are quiver electron velocities in the pump wave field and the daughter wave field, respectively. The first term being familiar one and derived in [11] for spatially homogeneous pump wave dominates if the inequality $\omega_0-2\omega>\omega_0 3k_0/\left(2\max\left(q_j\right)\right)$ holds. As this is not the case we consider, it will be neglected further that reduces the above equation to:

$$\rho_j\left(\vec{r};\Omega_j\right)\simeq-\frac{k_0u_{0x}}{4\pi\omega_0}q_{xj}q_{xp}\varphi_p\left[1+\frac{3}{2}\frac{\omega_0^2}{\Omega_j^2-\omega_{ce}^2}\right],\quad u_{0x}=\frac{|e|}{m_e}\frac{|\omega_e|}{\omega_0^2-\omega_{ce}^2}E_y.$$

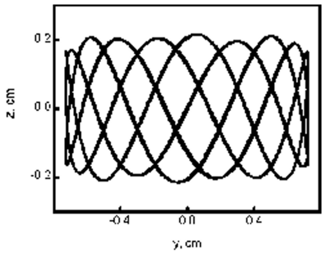

Fig. 2: The UH wave ray trajectory path demonstrating both its 2D trapping and the applicability of an adiabatic approximation. The same parameters as in figure 1, $P_0=400kW$.

3 THE REDUCED UH WAVES EQUATIONS

As was shown in [5] – [8] the PDI threshold decreases substantially when one of the daughter waves, IB wave in the particular case of these references, is trapped at least in x - direction. This is also possible for the UH wave if the turning point of its dispersion curve and the local maximum of the non-monotonous density profile, x_m, at the O-point of the magnetic island are close one to another and the convective losses along the magnetic field are small, *i.e.* at $q_z<<q_\perp$. Therefore, we seek a WKB solution of the system (2) in a vicinity of x_m and UH resonance

$$\phi_j^{(s)}=C_j\left(y,z,t\right)\exp\left(-i\int_{x_{j,1}^*}^{x}Q_s\left(\Omega_j,q_y,\xi\right)d\xi-iq_yy\right)\left[\int_{x_{j,1}^*}^{x_{j,2}^*}dx\frac{1}{\left|\upsilon_{g,s}^{(+)}\left(\Omega_j,x\right)\right|}+\frac{1}{\left|\upsilon_{g,s}^{(-)}\left(\Omega_j,x\right)\right|}\right]^{-1/2}\times$$
$$\left[\frac{\exp\left(-i\int_{x_{j,1}^*}^{x}\kappa_s\left(\Omega_j,q_y,\xi\right)d\xi\right)}{\sqrt{\upsilon_{g,s}^{(+)}\left(\Omega_j,x\right)}}+\frac{\exp\left(i\int_{x_{j,1}^*}^{x}\kappa_s\left(\Omega_j,q_y,\xi\right)d\xi\right)}{\sqrt{\upsilon_{g,s}^{(-)}\left(\Omega_j,x\right)}}\right],\tag{4}$$

$s=(k,l)$, $j=(1,2)$, $Q_s=\left(q_{x,s}^{(+)}+q_{x,s}^{(-)}\right)/2$, $\kappa_s=q_{x,s}^{(+)}-q_{x,s}^{(-)}$, $\upsilon_{g,j}^{(\pm)}=\partial D/\partial q_x\cdot\left[\partial D/\partial\Omega_j\right]^{-1}\Big|_{q_x^\pm}$, $\Omega_j=(\omega,\omega_0-\omega)$, $x_{j,1}^*$ and $x_{j,2}^*$ are solutions of equation $\upsilon_{g,s}^{(+)}\left(\Omega_j,x_{j,(1,2)}^*\right)=0$, $C_j\left(y,z,t\right)$ are slowly varying amplitudes and $q_x^\pm$ is the radial component of the wave vector

$$q_x^\pm\left(\omega,q_y,x\right)=\frac{\omega_{ce}}{\upsilon_{te}}\sqrt{-\varepsilon\pm\sqrt{\varepsilon^2-\frac{2\upsilon_{te}^2}{c^2}-\frac{q_y^2\upsilon_{te}^2}{\omega_{ce}^2}}}>>q_y\tag{5}$$

which obey the Born-Zommerfeld quantization conditions

$$\int_{x_{k,1}^*}^{x_{k,2}^*}\kappa_k\left(\omega\left(q_y^{k,l}\right),q_y^{k,l},\xi\right)d\xi=\pi k,\int_{x_{l,1}^*}^{x_{l,2}^*}\kappa_l\left(\omega_0-\omega\left(q_y^{k,l}\right),q_y^{k,l},\xi\right)d\xi=\pi l\tag{6}$$

Upon solving (6) we get $q_y^{k,l}$ and $\omega\left(q_y^{k,l}\right)$. The solution (4) with (5) and (6) having been found describes the UH waves trapped in a vicinity of the density maximum for which the convective losses in x direction are suppressed in full. We illustrate these waves in figure 1 where their 1D dispersion curves for the typical conditions of Textor experiments ($T_e = 500eV$, $\omega_0 = 140GHz$, $R_0 = 175cm$, $2\omega_{ce}\left(x_{ECR}\right) = \omega_0$, $\omega_0 / 2 = \sqrt{\omega_{ce}^2(x_m) + \omega_{pe}^2(x_m)}$, $x_{ECR} = -28cm$, $x_m = 28cm$, $w = 1cm$), aimed at

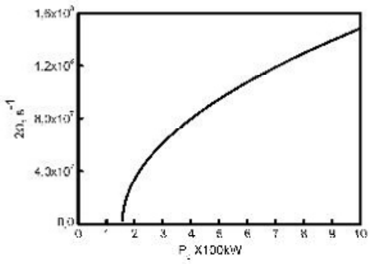

Fig. 3: The dependence of the growth rate on the power of the pump wave for $s = p = 1$. $T_e = 500eV$, $2\omega_{ce}\left(x_{ECR}\right) = \omega_0$, $P_0 = 600kW$, $w_y = w_z = 1cm$, $\omega = \omega_0 / 2$, $q_y = 0$, $k = l = 13$. The threshold of the PDI - $P_0^{th} = 160kW$.

neoclassical tearing mode control, with the actual density profile [9] are depicted. Then, we substitute (4) into (2), multiply the first line and second line in it by $\phi_1^{(k)*}$ and $\phi_2^{(l)*}$, and evaluate integration over x that yields

$$\begin{cases} \left[\dfrac{\partial}{\partial t} - U_k \dfrac{\partial}{\partial y} + i\Lambda_{yk} \dfrac{\partial^2}{\partial y^2} + i\Lambda_{zk} \dfrac{\partial^2}{\partial z^2} + \nu_{ei}\right] C_1\left(y,z,t\right) = \nu_k\left(y,z\right) C_2\left(y,z,t\right) \\ \left[\dfrac{\partial}{\partial t} + U_l \dfrac{\partial}{\partial y} - i\Lambda_{yl} \dfrac{\partial^2}{\partial y^2} - i\Lambda_{zl} \dfrac{\partial^2}{\partial z^2} + \nu_{ei}\right] C_2\left(y,z,t\right) = \nu_l^*\left(y,z\right) C_1\left(y,z,t\right) \end{cases} \tag{7}$$

where $\Delta_k\left\{f\right\} = \int\limits_{x_{k,1}^*}^{x_{k,2}^*} \left(\dfrac{f^+(x)}{\upsilon_{g,k}^{(+)}(\omega)} + \dfrac{f^-(x)}{\upsilon_{g,k}^{(-)}(\omega)} \right) dx \left[\int\limits_{x_{k,1}^*}^{x_{k,2}^*} \left(\dfrac{1}{\upsilon_{g,k}^{(+)}(\omega)} + \dfrac{1}{\upsilon_{g,k}^{(-)}(\omega)} \right) dx \right]^{-1}$, $\Lambda_{yk} = \Delta_k\left\{D_{qq}\right\} / \Delta_k\left\{D_\omega\right\}$, $\Lambda_{zk} = \Delta_k\left\{\eta\right\} / \Delta_k\left\{D_\omega\right\}$, $U_k = 2q_y^{k,l}\Lambda_{yk}$, $D_{qq}^{\pm} = \partial D\left(\omega, q_x, x\right) / \partial\left(q_x^2\right)\Big|_{q_{x,k}^{(\pm)}}$, $D_\omega^{\pm} = \partial D\left(\omega, q_x, x\right) / \partial\omega\Big|_{q_{x,k}^{(\pm)}}$, ν_{ei} is electron-ion collision frequency and $\nu_k\left(y,z\right)$ is overlapping integral, which defines parametric coupling of two plasmons:

$$\nu_k = -i \frac{\omega_{ce}^2}{\omega_0^2 - \omega_{ce}^2} \frac{a_i\left(y,z\right)}{2H_0} \left(1 + \frac{3}{2}\frac{\omega_0^2}{\omega_{pe}^2}\right) \times$$

$$\frac{1}{\Delta_k\left(D_\omega\right)} \left[\int_{x_{k,1}^*}^{x_{k,2}^*} dx \frac{1}{\left|\upsilon_{g,k}^{(+)}\left(\omega,x\right)\right|} + \frac{1}{\left|\upsilon_{g,k}^{(-)}\left(\omega,x\right)\right|} \right]^{-1/2} \left[\int_{x_{l,1}^*}^{x_{l,2}^*} dx \frac{1}{\left|\upsilon_{g,k}^{(+)}\left(\omega,x\right)\right|} + \frac{1}{\left|\upsilon_{g,k}^{(-)}\left(\omega,x\right)\right|} \right]^{-1/2} \times$$

$$\left[\int\limits_{\max(x_{k,1}^*, x_{l,1}^*)}^{\min(x_{k,2}^*, x_{l,2}^*)} dx \frac{q_{x,l}^{(-)}\left(\omega_0 - \omega, x\right) q_{x,k}^{(+)}\left(\omega, x\right) \exp\left[ik_0 x - i\int^x \left\{ q_{x,l}^{(-)}\left(\omega_0 - \omega, s\right) - q_{x,k}^{(+)}\left(\omega, s\right) \right\} ds \right]}{\sqrt{\upsilon_{g,l}^{(-)}\left(\omega_0 - \omega\right)} \sqrt{\upsilon_{g,k}^{(+)}\left(\omega\right)}} + \right.$$

$$\left. \int\limits_{\max(x_{k,1}^*, x_{l,1}^*)}^{\min(x_{k,2}^*, x_{l,2}^*)} dx \frac{q_{x,l}^{(+)}\left(\omega_0 - \omega, x\right) q_{x,k}^{(-)}\left(\omega, x\right) \exp\left[ik_0 x - i\int^x \left\{ q_{x,l}^{(+)}\left(\omega_0 - \omega, s\right) - q_{x,k}^{(-)}\left(\omega, s\right) \right\} ds \right]}{\sqrt{\upsilon_{g,l}^{(+)}\left(\omega_0 - \omega\right)} \sqrt{\upsilon_{g,k}^{(-)}\left(\omega\right)}} \right]$$

It deserves to be noted here that for high eigen-modes of the UH wave, *i.e.* at $k,l >> |k-l|$, $\Psi_k \simeq \Psi_l$, where $\Psi_k = \{U_k, \Lambda_{yk}, \Lambda_{zk}, \Xi_k, \gamma_k\}$. As was it shown for 1D case in [12, 13], the daughter waves

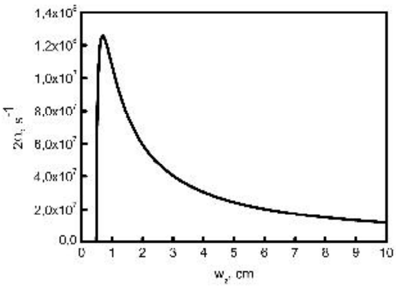

Figure 4. The dependence of the growth rate on the waist of the beam along the magnetic field. $s = p = 1$. $T_e = 500eV,\ \ x_{ECR} = -28cm,\ \ x_m = 28cm,\ \ 2\omega_{ce}(x_{ECR}) = \omega_0,$ $n(x_m) = 3.05\times10^{13}cm^{-3},\ \ P_0 = 600kW$, $w_y = 1cm,\ \ \omega = \omega_0/2,\ \ q_y = 0$, $k = l = 13$.

generated via the parametric decay of the finite-size pump wave beam and propagating in opposite directions can be nonlinearly localized by the beam. Below, we demonstrate both analytically and numerically the 2D daughter waves localization provided by the two-dimensional finite-size beam of the pump wave. For this purpose we seek a WKB solution of (7) in a form $\propto \exp[\Omega t + iS(y,z)]$ that yields the Eikonal equation

$$\tilde{D} = (\Omega + \nu_{ei})^2 + \left[U_k \frac{\partial S}{\partial y} + \Lambda_{yk}\left(\frac{\partial S}{\partial y}\right)^2 + \Lambda_{zk}\left(\frac{\partial S}{\partial z}\right)^2\right]^2 - |v_k(y,z)|^2 = 0 \qquad (8)$$

For the sake of simplicity and keeping in mind the typical Textor experimental conditions for which $U_k = 0$ (see figure 1 with its caption) we assume that the first term in the squire brackets in (8) is negligibly small compared to the last two there. One fast computational algorithm to approximate the solution to the eikonal equation is the ray-tracing procedure which gives the set of the second-order ordinary differential equations for the UH wave's front trajectory path

$$y'' = -F(y,z), z'' = -\frac{\Lambda_{zk}}{\Lambda_{yk}}F(y,z), F(y,z) = \frac{z\exp\left(-(y/w)^2 - (z/w)^2\right)}{\sqrt{\exp\left(-(y/w)^2 - (z/w)^2\right) - (\Omega+\nu_{ei})^2 \Big/ |v_k(0,0)|^2}} \qquad (9)$$

where the second derivatives are introduced over the dimensionless ray trajectory length. Though the system of the coupled equations (9) affords no separation of variables and thus analytical solution finding, it describes at $(\Omega+\nu_{ei})^2 \big/ |v_k(0,0)|^2 < 1$ the 2D finite behavior of the ray trajectory as is demonstrated in figure 2 for the Textor parameters (the same parameters as in figure 1, $U_k = 0$, $\Lambda_{zk}/\Lambda_{yk} = 17.35 >> 1$). We can see also that the wave propagates along the magnetic field (in z direction) much faster than in y direction that makes possible the approximate analytical description of the solution to (9) and its quantization by the adiabatic invariance method. Further we assume an artificial "rectangle" pump beam: $|v_k(y,z)|^2 = |v_k(0,0)|^2 \cdot H(y+w_y)H(w_y-y)$ $H(z+w_z)H(w_z-z)$ with $H(...)$ being Heaviside function. The consecutive quantization procedure (at first step in z direction assuming the coordinate y fixed and then in y direction) yields

$$2\Omega = -2\nu_{ei} + 2\sqrt{|v_k(0,0)|^2 - \left[\pi^2 s^2/(2w_y)^2 \cdot \Lambda_{yk} + \pi^2 p^2/(2w_z)^2 \cdot \Lambda_{zk}\right]^2} \qquad (10)$$

Then, setting $\Omega = 0$ we obtain for the most dangerous fundamental mode $p = s = 1$ the threshold of the PDI in the form

$$\left|v_k(0,0)\right|^2 \left\{P_0^{th}\right\} = \frac{\pi^4}{16}\left(\frac{\Lambda_{yk}}{w_y^2} + \frac{\Lambda_{zk}}{w_z^2}\right)^2 + \nu_{ei}^2 \tag{11}$$

The dependence of the growth rate ($s = p = 1$) given in (10) on the pump wave power is illustrated in figure 3 for the typical Textor parameters. As we can see the threshold of the PDI is $P_0^{th} = 160kW$ and the growth rate at the power range of the pump wave $200 \div 600kW$ used in Textor is high enough $2\Omega \geq \omega_{ci}$ to make this parametric decay very dangerous. In figure 4 the dependence of the growth rate (10) on the beam waist along the magnetic field is shown as well. We can see there that this dependence possesses the cut-off at the small pump wave beam waist when the diffraction losses of the daughter waves along the magnetic field start to dominate over the non-linear pumping. At the high beam waist the diffraction losses play no role and the growth rate decreases with increasing beam waist proportionally to the pump field amplitude at constant power. This behavior is the same as for the homogeneous theory growth rate.

4 CONCLUSIONS

We analyzed the parametric decay of the 2nd harmonic X-mode wave into two short wave-length UH plasmons which propagate in opposite directions. The possibility of the 3D localization of both the UH decay waves due to local maximum of the density in the O-point of the island (in the radial direction) and due to the finite-size pump wave beam (along the magnetic surface) was shown to lead to the excitation of the absolute PDI. We derived explicitly for “rectangle” pump beam the growth rate of the PDI and the threshold of the absolute PDI which for the typical Textor parameters is in the power range of a couple hundreds kW that drastically smaller than that provided by the standard theory [1] – [3].

Work supported by RFBR grants 12-02-90003-Bel, 10-02-00887, NWO-RFBR Centre of Excellence on Fusion Physics and Technology (grant 047.018.002), the RAS Presidium program №12 and the RF government grant № 11.G34.31.0041

1. A. G. Litvak et al., *Phys. Fluids* **B 5**, 4347 (1993)
2. M. Porkolab et al., *Nucl. Fusion* **28**, 239 (1988)
3. B. I. Cohen et al., *Rev. Mod. Phys.* **63**, 949 (1991)
4. E. Westerhof et al., *Phys. Rev. Lett.* **103**, 125001 (2009)
5. E.Z. Gusakov et al., *JETP Letters* **91**, 655 (2010)
6. E.Z. Gusakov et al., *Phys. Rev. Lett.* **105**, 115003 (2010)
7. E.Z. Gusakov et al., *Nuclear Fusion* **51**, 073028 (2011)
8. E. Z. Gusakov et al., *JETP Letters* **94**, 277 (2011)
9. M.Yu. Kantor et al., *PPCF* **51**, 055002 (2009)
10. S.K. Nielsen, M. Salewski, E. Westerhof *private communication* (2011)
11. V.P. Silin, *Parametric Action of High Power Radiation on Plasma* [in Rus], (1973).
12. L.M. Gorbunov, *Sov. Phys.-JETP* **35**, 1119 (1972)
13. L.M. Gorbunov, *Sov. Phys.- JETP* **40**, 689 (1975)